Grassland canopy vertical structure retrieval from multi-angular and multi-temporal fine quad-pod Radarsat-2 images

Zhaoqin Li[1,2] and Xulin Guo[1]

1 Geography and Planning, University of Saskatchewan, xulin.guo@usask.ca

2 Global Institute for Water Security, University of Saskatchewan, Saskatoon, SK, zhaoqin.li@usask.ca

Abstract

Canopy vertical structure described by leaf area index (LAI) and canopy height is an important input for ecology, climatology, hydrology, and biochemistry modelling and an essential measurement for wildlife habitat suitability. However, accuracy of LAI and canopy height estimation with optical remote sensing in mixed prairie grasslands is highly influenced by large amounts of dead vegetation, biological soil crust, and bare soil. This study explored the potential of Radarsat-2 data to retrieve LAI and canopy height. In total eight fine quad-pod Radarsat-2 images with incidence angles from 20.9° to 46.5° were acquired from June 15 to July 9, 2014 in Grasslands National Park, Canada. Co-polarization ratio (HH/VV), cross-polarization ratios (HV/HH; HV/VV; VH/HH; and VH/VV), Radar Vegetation Index, Depolarization ratio (σ_vh^0 (dB)-σ_vv^0 (dB)), and the Freeman-Durden decomposition components were used to establish relationships with ground measured LAI and canopy height. Results indicate that incidence angle is critical for both LAI and canopy height estimation with the best result (r2=0.70 and 0.69 respectively) achieved using FQ23 (41.9°-43.3°) data. Co-polarization ratio (HH/VV) is the most suitable parameter for LAI and canopy height estimation.

Background and Relevance

Leaf area index (LAI) and canopy height are two indicators of canopy vertical structure. They are key parameters in the land surface-atmosphere interaction models (Knyazikhin et al., 1998). LAI is important in modelling because it controls photosynthesis and respiration rates of vegetation, the interception of precipitation, and the portioning of energy available to sensible and latent heat(Wilson et al., 2002). Canopy height is vital for it partially determines surface roughness and thus affects the energy balance between land surface and atmosphere (Raupach, 1994). In addition, LAI and canopy height are two essential measurements for evaluating suitability of wildlife habitat (McDermid et al., 2009), and monitoring grassland vegetation growth and assessing grassland health (Chen et al., 2013).

The availability of temporally and spatially explicit remote sensing data makes it possible to quantify temporal and spatial variations of LAI and canopy height that are essential for modelling (Nelson et al., 2009). Since the advent of Landsat Multispectral Scanner (MSS) in 1972, numerous studies have been conducted to quantify LAI with optical remote sensing approaches (Propastin and Kappas, 2009; Tang et al., 2016). However, accuracy of LAI estimation from optical remote sensing data in semiarid mixed grassland is limited by presence of considerable amount of dead vegetation, biological soil crust (BSC), and bare soil (Li et al., 2014). Although efforts have been made to improve LAI estimation by developing a litter-corrected hyperspectral index (He et al., 2006) and taking spatial and temporal variations of LAI into account (Li and

Guo, 2013) in such mixed prairie grasslands, the achieved r2 values of LAI were still not beyond 0.60.

Radar backscattering coefficient data has been well related to LAI in croplands (Ulaby et al., 1984), and since then considerable research has been conducted on quantifying LAI in forests and croplands (e.g., Manninen et al., 2005; Mattia et al., 2003) . More recently, C- band and X-band synthetic aperture radar (SAR) data have been used in monitoring irrigated grasslands (Baghdadi et al., 2016; Hajj et al., 2014) and mapping Western Canada grassland (Buckley and Smith, 2010; Smith and Buckley, 2011). However, limited research has been conducted on quantifying grassland biophysical parameters, including LAI in mixed prairie grassland. In addition, canopy height estimation in grasslands with remote sensing approaches has not been documented in the literature, to our knowledge, although LiDAR data, SAR data, and SAR interferometry techniques have been widely used for canopy height estimation in forests (Chirici et al., 2016; Ningthoujam et al., 2016; Sexton et al., 2009).

This paper investigated potential of polarimetric Radarsat-2 images for LAI and canopy retrieval in semiarid mixed grassland. Specifically, this study investigated the influence of incidence angle of Radarsat -2 images on LAI and canopy height estimation. The most suitable SAR parameters including the co-polarization ratio, cross-polarization ratios, depolarization ratio, radar vegetation index (RVI), and Freeman-Durden decomposition parameters were also determined.

Methods and Data

Field data

Field data including leaf area index (LAI) and canopy height were measured in the growing season of 2014 (June 20- July 02) in Grasslands National Park (GNP, 49.10°N, 106.89°W), Canada (Figure 1). GNP, as a portion of northern mixed grass prairie, is characterized by large amount of dead vegetation due to the lack of fire and light grazing. The presence of dead vegetation, biological soil crust (BSC), and bare soil exert a significant effect on LAI estimation and canopy height estimation using optical remote sensing data. Major soil types in GNP are Chernozemic and solonetzic soils (Fargey et al., 2000). Vegetation communities consisting of upland, valley, and slope were identified based on topography. Upland vegetation communities are dominated by speargrass - blue grama (Stipa comate - Bouteloua gracilis) and western wheatgrass - sedge (Agropyron smithii - Carex sp.)(Li and Guo, 2014). Western wheatgrass and silver sagebrush (Agropyron smithi - Artemesia cana) are the main species in valley vegetation communities (Li and Guo, 2014). Slope land communities hold the main vegetation species of both valley and upland. Crested wheatgrass (Agropyron cristatum) and smooth brome (Bromus inermis) communities are the two main disturbed communities.

LAI and canopy height were measured using a LAI-2000 plant canopy analyzer (Licor, Lincoln,USA) and a ruler, respectively, in the fourteen sites randomly set up in upland, valley, slope land, and disturbed communities (Figure 1). The measurements were taken within a 50 × 50 cm quadrat at 10 m intervals over two 100 m long transects crossing at right angles at each site, yielding 20 measurements at each site. The 20 measurements of LAI and canopy height at each site were averaged respectively for statistical analysis to avoid spatial autocorrelation. Note that the measured LAI is not only from green vegetation, but also include standing dead vegetation. Canopy height was measured as the aboveground height of the majority vegetation within each sampling quadrat. The average, maximum, minimum, and standard deviation of LAI and canopy height among the sampling sites are described in Table 1, and a LAI-canopy height scatter plot is shown in Figure 2.

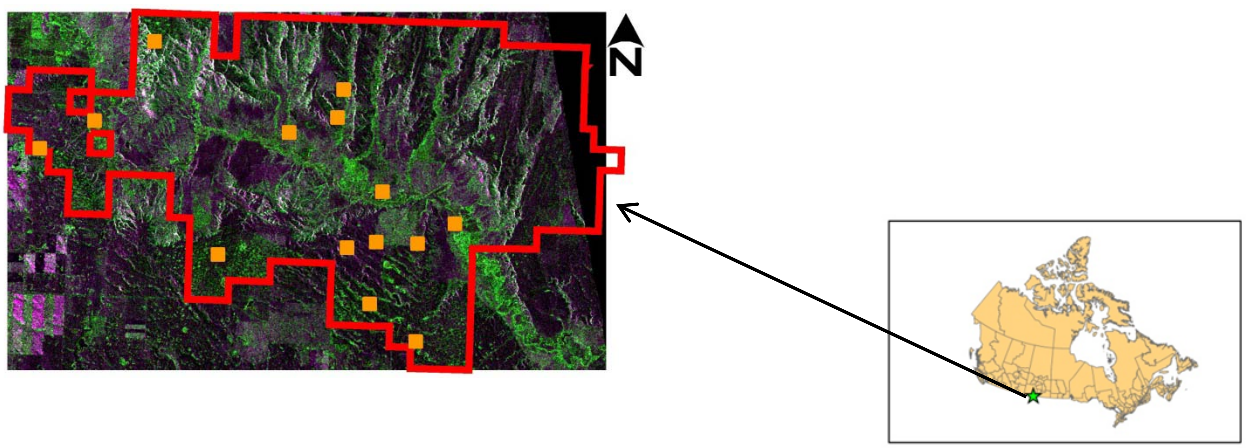

Figure 1 The geographic location of the study site with distribution of sampling sites in 2014 (The background is Radarsat-2 FQ1 image acquired on Jun 02, 2014; and RGB was assigned as HH, HV, and VV backscatter coefficients)

Table 1 Descriptive analysis of leaf area index (LAI) and canopy height sampled in the summer of 2014

Statistic Description	Leaf Area Index (m^2/m^2)	Canopy Height (cm)
Average	1.8	28
Maximum	3.1	39
Minimum	0.9	21
Standard Deviation	0.7	6

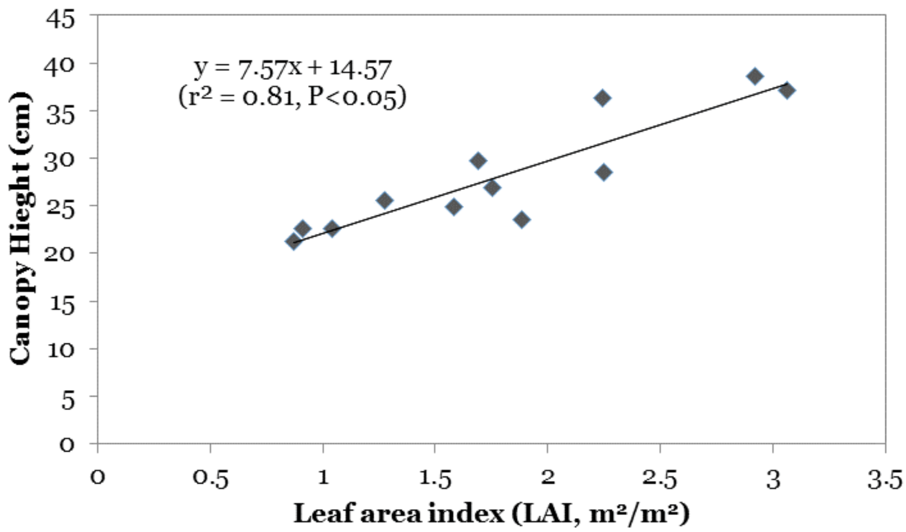

Figure 2. The relationship between leaf area index (LAI) and canopy height derived from the field measurements of 2014

Images

In total eight Radarsat-2 fine quad-pod single-look complex (SLC) images acquired from Jun 15 through July 09, 2014 were used in this study (Table 2). The incidence angles of the images range from 20.9° to 46.5° and the spatial resolution is 5 m. Precipitation within three days and 12 hours prior to acquisition (Table 2) were downloaded from the Environment Canada website to check the effects of rain on the data quality. Raindrops and dew after raining will enlarge canopy water content and thus increase backscatter. Based on the environmental data in Table 2, the quality of those images was not directly compromised by dew or raindrop. However, the FQ12 image on June 18 and the FQ5 image on June 19 may be influenced by canopy and soil moisture content.

Table 2 The Radarsat-2 images used in this study

Month-Day-2014	Beam mode	Incident angle range (°)	Spatial Resolution X (m) × Y (m)	Daily Precipitation (mm)	3 days' precipitation (mm)
Jun 15	FQ23	41.9-43.3	4.73 × 4.94	0.2	9.6
Jun 18	FQ12	31.5-32.9	4.73 × 4.96	24.9	89
Jun 19	FQ5	23.4-25.3	4.73 × 4.97	0.4	113.7
Jun 28	*FQ3	20.9-22.9	4.73 × 5.33	0.7	20
Jul 02	FQ27	45.2-46.5	4.73 × 4.85	0	2.7
Jul 05	*FQ7	25.8-27.6	4.73 × 4.74	0	0
Jul 06	FQ10	29.2-30.9	4.73 × 5.18	0	0
Jul 09	FQ23	41.9-43.3	4.73 × 4.94	0	4.5

The Radarsat-2 images were pre-processed and then SAR parameters were retrieved following standard procedures (Figure 3). Orthorectification of the Radarsat-2 images was conducted using the Radar Specific Model and Advanced Spaceborne Thermal Emission and Reflection Radiometer (ASTER) Global Digital Elevation Model Version 2 (GDEM V2) in the Radar Ortho Suite of PCI Geomatica 2015. After orthorectification, speckle noise of the images was filtered using the boxcar filter (5×5 pixels) approach. The boxcar method is commonly used when the features on the image are relatively homogenous and loss of spatial resolution is not a concern (Lee et al., 2015).

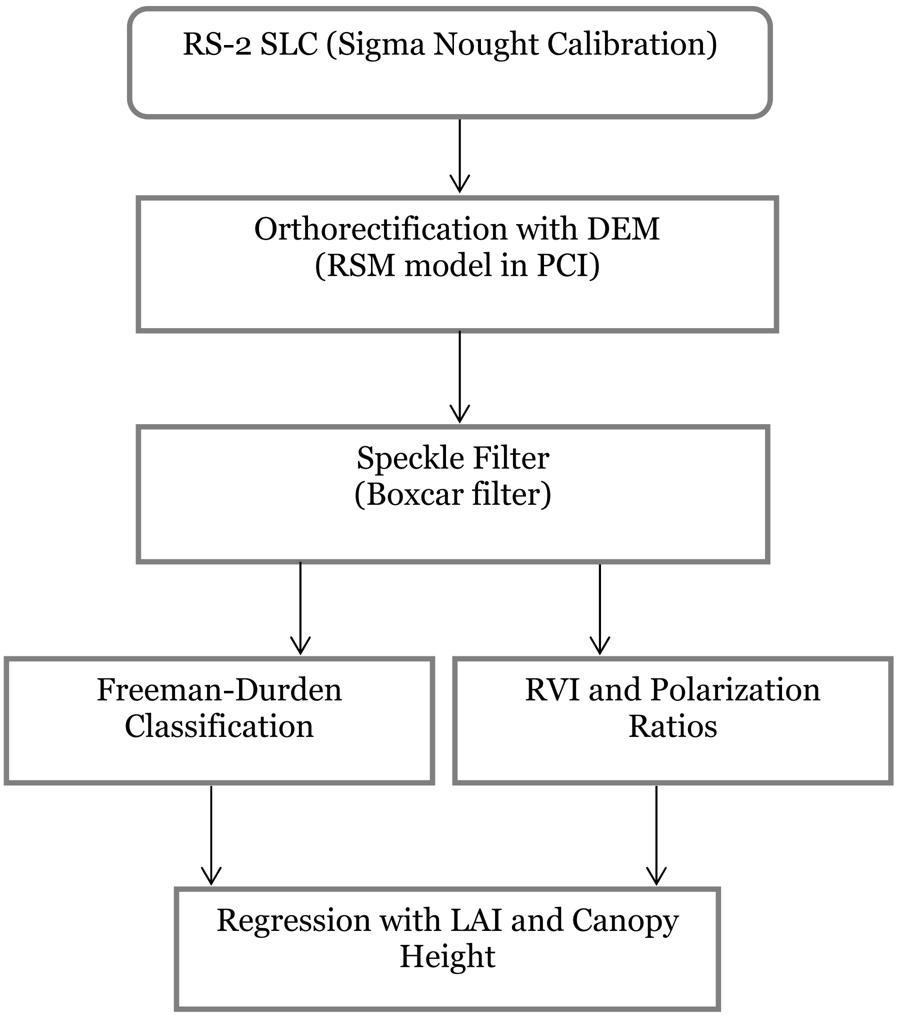

Figure 3. The flow chart of Radarsat-2 processing for leaf area index (LAI) and canopy height estimation

Methods

After speckle removal, SAR parameters were retrieved from the Radarsat-2 images for quantifying LAI and canopy height through simple linear regression. The retrieved SAR parameters were vegetation scattering (dipole scattering), double bounce (dihedral scattering), and surface scattering (Bragg scattering) (Freeman and Durden, 1998), co-polarization ratio (HH/VV), cross-polarization ratios (HV/HH, HV/VV ,VH/HH, and VH/VV), depolarization ratio, and Radar Vegetation Index (RVI). Depolarization ratio (x_v) that is sensitive to surface roughness (Gherboudj et al., 2011) was calculated from Eq. (1), and RVI which is sensitive to biomass variation (Kim and van Zyl, 2009) was calculated from Eq. (2).

$$x_v = \sigma_{VH}(dB) - \sigma_{VV}(dB) \quad (1)$$

Where σ_{VH} and σ_{VV} are the VH cross-polarization and VV co-polarization backscatter coefficients in decibel (dB) respectively.

$$RVI = \frac{8\sigma_{HV}}{\sigma_{HH} + \sigma_{VV} + 2\sigma_{HV}} \quad (2)$$

Where σ_{HV} is the cross-polarization backscattering and σ_{HH} and σ_{vv} are the co-polarization backscattering coefficient in power unit.

To match the 100 × 100 m sampling site size, SAR parameters at each sampling site were retrieved within a 19 × 19 pixel window size and then averaged to represent the sampling site. Outliers of LAI and canopy height were checked at the quadrat level based on statistical analysis and the photos taken at the quadrats. After outlier removal, the sample number for analysis of most images is 12, expect for the July 5 image that only covered 10 sampling sites.

Results and Discussion

SAR parameters for canopy height estimation

The r^2 values of SAR parameters for canopy height estimation are presented in Table 3. The best estimation on canopy height was achieved by the July 9 FQ23 image with an r^2 value of 0.69, followed by an r^2 value of 0.65 using the June 15 FQ23 image. The July 2 FQ27 image could significantly account for 50% variations in canopy height. From the first image acquisition on June 15 to the last one on July 9, canopy height gradually increased until reach the growing peak in early July. Considering canopy height was measured during June 20 to July 2, it is not surprisingly to see a slightly better performance of the July 9 FQ23 image than that of the June 15 Q23 image. The FQ27 image on July 2 was not good as the June 15 FQ23 image, which indicated incidence angle of the image was more critical than acquisition time for canopy height estimation in grasslands.

The best SAR parameter for canopy height estimation is the co-polarization ratio (HH/VV). The SAR parameters including the cross-polarization ratio (HV/VV and VH/VV), de-polarization ratio, and vegetation scattering also demonstrated certain ability for canopy height estimation. Nonetheless, they were not consistently good as the HH/VV for the three shallow incidence angle images including the June 15 and July 09 FQ23 images and the July 2 FQ27 images. The other SAR parameters, including RVI, HV/HH, VH/HH, surface scattering, and multiple scattering did not demonstrate potential for canopy height estimation. Conventionally, HV and VH backscatter is assumed to be similar (Moran et al., 2012); however, the difference in the r^2 values on canopy height estimation using the HV/HH and VH/HH, or the HV/VV and VH/VV can be large. For example, using the July 9 FQ23 image, the r^2 value (0.58) of HV/VV is much larger than that (0.40) of the VH/VV.

Table 3 The r^2 values of Radarsat-2 parameters for canopy height estimation

Date	Beam mode	RVI	HH/ VV	HV/ HH	HV/ VV	VH/ HH	VH/ VV	D-ratio	V scatter	S scatter	M scatter
Jun 15	FQ23	0.17	0.65*	0.05	0.35	0	0.31	0.26	0.64*	0	0.35
Jun18	FQ12	0.14	0.25	0.05	0.40	0.05	0.43*	0.38	0.14	0.15	0.04
Jun19	FQ5	0.03	0.42*	0	0.07	0	0.08	0.22	0.38	0.12	0.12
Jun28	FQ3	0.01	0.13	0	0.02	0	0.04	0.07	0.33	0	0.14
Jul02	FQ27	0	0.5*	0.09	0.17	0.07	0.23	0.24	0.45*	0.01	0.35
Jul05	FQ7	0.29	0.26	0.22	0.33	0.37	0.42*	0.44*	0.20	0.03	0.08
Jul06	FQ10	0.20	0.33	0.09	0.31	0.02	0.21	0.21	0.31	0	0.20
Jul09	FQ23	0.32	0.69*	0.09	0.58*	0	0.40	0.35	0.20	0.15	0.22

*denotes the statistical significance at the 0.05 level. D-ratio is depolarization ratio; V, S, and M scatter represents volume scattering, surface scattering, and multiple scattering respectively.

SAR parameters for LAI

The r2 values for LAI estimation from the retrieved SAR parameters are presented in Table 4. The largest r^2 value is 0.70 for LAI estimation which was achieved using the FQ23 image on June 15. The July 2 FQ27 image also demonstrated good performance on LAI estimation with an r2 value of 0.64. The FQ7 image on July 5 and FQ5 image on June 19 also demonstrated potential for LAI estimation. However, the SAR parameters retrieved from the FQ12 image on June 18 and the FQ10 image on July 6 did not show a promise for LAI estimation. The best r^2 value (0.70) of LAI estimation in this study is much larger than that (0.55) using hyperspectral vegetation indices (He et al., 2006) and that of 0.48 using multispectral Landsat images (Xu, 2016) in the same study area.

The co-polarization ratio (HH/VV) is the best SAR parameter for LAI estimation. The other potential SAR parameters for LAI estimation are the cross-polarization ratio (HV/VV, VH/VV, and VH/HH), de-polarization ratio, RVI, and vegetation scattering. The retrieved SAR parameters including RVI, HV/HH, surface scattering, and multiple scattering did not contain useful information for LAI estimation. Similar to canopy height estimation, using the HV/HH and VH/HH, or the HV/VV and VH/VV can also lead to fairly large difference in the r^2 values, although HV and VH are conventionally assumed to be similar (Moran et al., 2012). Using the July 9 FQ23 image as an example, the r^2 value of the HV/VV for LAI estimation is 0.58, while of the VH/VV is only 0.33.

Table 4 The r^2 values of Radarsat-2 parameters for leaf area index (LAI) estimation

Date	Beam	RVI	HH/	HV/	HV/	VH/	VH/	D-	V	S	M

	mode		VV	HH	VV	HH	VV	ratio	scatter	scatter	scatter
Jun15	FQ23	0.13	**0.70***	0.03	0.31	0	0.27	0.22	0.40*	0	0.21
Jun18	FQ12	0.07	0.27	0.01	0.30	0.02	0.33	0.29	0.07	0.24	0.11
Jun19	FQ5	0.08	0.48*	0.03	0.15	0.05	0.19	0.34*	0.48*	0.15	0.09
Jun28	FQ3	0	0.20	0	0	0	0.01	0.04	0.10	0	0.07
Jul02	FQ27	0	0.64*	0.19	0.14	0.16	0.21	0.22	0.23	0	0.29
Jul05	FQ7	0.40*	0.28	0.29	0.47*	0.48*	0.58*	0.57*	0.02	0.02	0
Jul06	FQ10	0.14	0.21	0.08	0.20	0.03	0.15	0.16	0.15	0.02	0.15
Jul09	FQ23	0.30	0.59*	0.08	0.54*	0	0.33	0.28	0.07	0.13	0.07

*denotes the statistical significance at the 0.05 level. D-ratio is depolarization ratio; V, S, and M scatter represents volume scattering, surface scattering, and multiple scattering respectively.

The good performance on canopy height and LAI estimation of large incidence angle images including the FQ23 and FQ27 images possibly attributes to the fact that the larger incidence angle, the smaller penetration capability to surface, and thus backscatter coefficients of the images are more controlled by vegetation rather than surface. The small incidence angle image, such as the FQ3 image, could not capture the variations in canopy structure, possibly because the contribution to the backscattering coefficient was more from the surface instead of the canopy due to the high penetration capability. The inverse relationship between incidence angle and penetration may also explain the potential of the FQ5 and FQ7 images and the inferiority of the FQ10 and FQ12 images for canopy structure estimation in grasslands. However, a theoretical SAR backscattering model is needed in the future study to fully understand how incidence angle, frequency, spatial resolution, and temporal revisit etc. of the SAR images affect canopy structure estimation in grassland ecosystems.

Conclusions

This study investigated multi-angular and multi-polarization Radarsat-2 images for quantifying canopy structure parameters including canopy height and leaf area index in semiarid mixed prairie grasslands where application of optical remote sensing data is hindered by the contribution of dead vegetation, biological soil crust (BSC), and bare soil to the spectra. Research concluded that incidence angle is critical for both LAI and canopy height estimation and the best canopy structure estimation was achieved by the FQ23 (41.9°-43.3°) image. The co-polarization ratio (HH/VV) is the most suitable parameter for LAI and canopy height estimation.

Acknowledgements

This research was financially supported by a Natural Sciences and Engineering Research Council of Canada (NSERC) Discovery Grant (Dr. X. Guo) and NSERC Alexander Graham Bell Canada Graduate Scholarship (Z. Li). Thanks also go to Dr. Dandan Xu, Tengfei Cui, Meng Li, Bin Lu, and James Liu for field data collection. The ASTER-GDEM data is a product of the Ministry of Economy, Trade and Industry (METI) of Japan and the United States National Aeronautics and Space Administration (NASA). We also thank the Canadian Space Agency and the Canada Centre for Remote Sensing for providing RADARSAT-2 data through the Science and Operational Applications Research—Education initiative (SOAR-E) program.

References

Baghdadi, N.N., El Hajj, M., Zribi, M., Fayad, I., 2016. Coupling SAR C-band and optical data for soil moisture and leaf area index retrieval over irrigated grasslands. IEEE Journal of Selected Topics in Applied Earth Observations and Remote Sensing 9, 1229-1243.

Buckley, J.R., Smith, A.M., 2010. Monitoring grasslands with RADARSAT 2 quad-pol imagery, Geoscience and Remote Sensing Symposium (IGARSS), 2010 IEEE International. IEEE, pp. 3090-3093.

Chen, G., Fan, W., Deng, M., 2013. Monitoring of degrading grassland based on HJ-1A-HSI image, 2013 IEEE International Geoscience and Remote Sensing Symposium-IGARSS. IEEE, pp. 800-803.

Chirici, G., McRoberts, R.E., Fattorini, L., Mura, M., Marchetti, M., 2016. Comparing echo-based and canopy height model-based metrics for enhancing estimation of forest aboveground biomass in a model-assisted framework. Remote Sensing of Environment 174, 1-9.

Fargey, K.S., Larson, S.D., Grant, S.J., Fargey, P., Schmidt, C. 2000. Grasslands National Park field guide: Prairie wind & silver sage - friends of grasslands Inc.

Freeman, A., Durden, S.L., 1998. A three-component scattering model for polarimetric SAR data. IEEE Transactions on Geoscience and Remote Sensing 36, 963-973.

Gherboudj, I., Magagi, R., Berg, A.A., Toth, B., 2011. Soil moisture retrieval over agricultural fields from multi-polarized and multi-angular RADARSAT-2 SAR data. Remote Sensing of Environment 115, 33-43.

Hajj, M.E., Baghdadi, N., Belaud, G., Zribi, M., Cheviron, B., Courault, D., Hagolle, O., Charron, F., 2014. Irrigated grassland monitoring using a time series of terraSAR-X and COSMO-skyMed X-Band SAR Data. Remote Sensing 6, 10002-10032.

He, Y., Guo, X., Wilmshurst, J., 2006. Studying mixed grassland ecosystems I: suitable hyperspectral vegetation indices. Canadian Journal of Remote Sensing 32, 98-107.

Kim, Y., van Zyl, J.J., 2009. A time-series approach to estimate soil moisture using polarimetric radar data. IEEE Transactions on Geoscience and Remote Sensing 47, 2519-2527.

Knyazikhin, Y., Martonchik, J., Myneni, R., Diner, D., Running, S., 1998. Synergistic algorithm for estimating vegetation canopy leaf area index and fraction of absorbed photosynthetically active radiation from MODIS and MISR data. Journal of Geophysical Research 103, 32257-32275.

Lee, J.-S., Ainsworth, T.L., Wang, Y., Chen, K.-S., 2015. Polarimetric SAR speckle filtering and the extended sigma filter. IEEE Transactions on Geoscience and Remote Sensing 53, 1150-1160.

Li, Z., Guo, X., 2013. Leaf area index estimation in semiarid mixed grassland by considering both temporal and spatial variations. Journal of Applied Remote Sensing 7, 073567-073567.

Li, Z., Guo, X., 2014. Topographic Effects on Vegetation Biomass in Semiarid Mixed Grassland under Climate Change Using AVHRR NDVI Data. British Journal of Environment and Climate Change 4, 229.
Li, Z., Xu, D., Guo, X., 2014. Remote sensing of ecosystem health: opportunities, challenges, and future perspectives. Sensors 14, 21117-21139.
Manninen, T., Stenberg, P., Rautiainen, M., Voipio, P., Smolander, H., 2005. Leaf area index estimation of boreal forest using ENVISAT ASAR. IEEE Transactions on Geoscience and Remote Sensing 43, 2627-2635.
Mattia, F., Le Toan, T., Picard, G., Posa, F.I., D'Alessio, A., Notarnicola, C., Gatti, A.M., Rinaldi, M., Satalino, G., Pasquariello, G., 2003. Multitemporal C-band radar measurements on wheat fields. IEEE Transactions on Geoscience and Remote Sensing 41, 1551-1560.
McDermid, G., Hall, R., Sanchez-Azofeifa, G., Franklin, S., Stenhouse, G., Kobliuk, T., LeDrew, E., 2009. Remote sensing and forest inventory for wildlife habitat assessment. Forest Ecology and Management 257, 2262-2269.
Moran, M.S., Alonso, L., Moreno, J.F., Mateo, M.P.C., De La Cruz, D.F., Montoro, A., 2012. A RADARSAT-2 quad-polarized time series for monitoring crop and soil conditions in Barrax, Spain. IEEE Transactions on Geoscience and Remote Sensing 50, 1057-1070.
Nelson, E., Mendoza, G., Regetz, J., Polasky, S., Tallis, H., Cameron, D., Chan, K., Daily, G.C., Goldstein, J., Kareiva, P.M., 2009. Modeling multiple ecosystem services, biodiversity conservation, commodity production, and tradeoffs at landscape scales. Frontiers in Ecology and the Environment 7, 4-11.
Ningthoujam, R.K., Balzter, H., Tansey, K., Morrison, K., Johnson, S., Gerard, F., George, C., Malhi, Y., Burbidge, G., Doody, S., 2016. Airborne S-band SAR for forest biophysical retrieval in temperate mixed forests of the UK. Remote Sensing 8, 609.
Propastin, P., Kappas, M., 2009. Integration of Landsat ETM+ Data with Field Measurements for Mapping Leaf Area Index in the Grasslands of Central Kazakhstan. GIScience & Remote Sensing 46, 212-231.
Raupach, M., 1994. Simplified expressions for vegetation roughness length and zero-plane displacement as functions of canopy height and area index. Boundary-Layer Meteorology 71, 211-216.
Sexton, J.O., Bax, T., Siqueira, P., Swenson, J.J., Hensley, S., 2009. A comparison of lidar, radar, and field measurements of canopy height in pine and hardwood forests of southeastern North America. Forest Ecology and Management 257, 1136-1147.
Smith, A.M., Buckley, J.R., 2011. Investigating RADARSAT-2 as a tool for monitoring grassland in western Canada. Canadian Journal of Remote Sensing 37, 93-102.
Tang, H., Ganguly, S., Zhang, G., Hofton, M., Nelson, R., Dubayah, R., 2016. Characterizing leaf area index (LAI) and vertical foliage profile (VFP) over the United States. Biogeosciences 13, 239.
Ulaby, F., Allen, C., Eger, G., Kanemasu, E., 1984. Relating the microwave backscattering coefficient to leaf area index. Remote Sensing of Environment 14, 113-133.
Ulaby, F.T., Kouyate, F., Brisco, B., Williams, T.L., 1986. Textural infornation in SAR images. IEEE Transactions on Geoscience and Remote Sensing, 235-245.
Wilson, K.B., Baldocchi, D.D., Aubinet, M., Berbigier, P., Bernhofer, C., Dolman, H., Falge, E., Field, C., Goldstein, A., Granier, A., 2002. Energy partitioning between latent and sensible heat flux during the warm season at FLUXNET sites. Water Resources Research 38.
Xu, D., 2016. Measuring grassland response to management using optical remote sensing. PhD thesis. University of Saskatchewan.Please refer to APA guidelines for the use of references and citations.